ULTRA SENSITIVE LORENTZ FORCE MEMS MAGNETOMETER WITH PICO-TESLA LIMIT OF DETECTION

Varun Kumar, Mohammad Mahdavi, Xiaobo Guo, Emad Mehdizadeh and Siavash Pourkamali
Electrical Engineering Department, University of Texas at Dallas, Richardson, USA

ABSTRACT

This work presents ultra-high sensitivities for Lorentz Force resonant MEMS magnetometers enabled by internal thermal-piezoresistive vibration amplification. Up to 2400X increase in sensitivity has been demonstrated by tuning the resonator bias current to maximize its internal amplification factor boosting the effective Quality Factor (Q) from its intrinsic value of 680 to 1.14×10^6 (1675X amplification). For a bias current of 7.245mA, where the sensitivity of the device is maximum (2.107mV/nT), the noise floor is measured to be as low as 2.8 pT/√Hz. This is by far the most sensitive MEMS Lorentz force magnetometer demonstrated to date.

INTRODUCTION

Magnetic sensors have found their way into a variety of applications such as Magneto-encephalography [1], magnetic anomaly detection, mineral prospecting [2], munitions fusing, magnetic compass [3], automotive sensors, respiratory measurements [4], and magnetic memory readout. Depending on the magnitude of the magnetic field to be detected, a number of techniques currently exist. Devices based on existing techniques include Hall Effect Sensors (μT-T), anisotropic magnetoresistance sensors (AMR- nT-mT), Optical Fiber [5] & Fluxgate sensors (nT-mT). Search Coils [6] and SQUIDS can detect extremely small fields (down to femto-Tesla) however, Search coils are quite bulky and unable to detect static magnetic fields, and SQUIDS on the other hand require cryogenic cooling and have high sensitivity to electromagnetic interference, thus requiring a sophisticated infrastructure (liquid helium supply, glass-fiber-reinforced epoxy Dewar vessels, and electromagnetic shielding). MEMS Magnetometers have an edge over the abovementioned conventional counterparts due to their small size, low cost, lower power consumption and operation simplicity. Such properties offer unrivalled advantages, especially when it comes to medical applications, such as magneto-encephalography, where compact arrays of ultra-sensitive sensors are desirable. Resonant Lorentz force magnetometers are one of the most common categories of MEMS magnetometers that can be implemented in silicon without the need for any special magnetic materials, and unlike magneto-resistive and fluxgate sensors they are free from hysteresis. Such devices take advantage of high Q microscale resonant structures to turn small Lorentz forces into measurable vibration amplitudes. Resonant Lorentz force magnetometers are typically operated at frequencies in the tens to hundreds of kHz, which helps significantly suppress the low frequency noise.

Limit of detection (LOD) for Lorentz force resonant MEMS magnetometers are typically in the lower μT to higher nT range, which is many orders of magnitude higher than the required LOD for most medical applications (pT to aT). A number of approaches have been reported to increase the sensitivity of such sensors. This includes using novel topologies [7], electronic tunneling [8] and parametric amplification [9]. In [9], the force-to-displacement transduction of a resonant sensor was increased via artificially increasing the resonator quality factor through modulation of the spring constant of the device at twice its natural frequency. Sensitivity was parametrically amplified by 50 folds using this approach to 39nT/√Hz. However, operation of parametrically amplified devices as practical sensors is quite challenging due to sophistication of supporting electronics. In this work, the previously demonstrated internal thermal-piezoresistive amplification [12] within the micromechanical silicon structure is used to reach much larger vibration amplitudes for the same magnetic actuation, consequently achieving much higher sensitivity [10] [11].

Internal Amplification

Internal thermal-piezoresistive amplification in resonant structures comprising of longitudinally stressed beams has been previously demonstrated [10] [11] [12]. As the resonator vibrates, the alternating tensile and compressive stress in the longitudinally stressed beams modulates their electrical resistance due to the piezoresistive effect. Modulation of electrical resistance, while maintaining a constant bias current or voltage across the beam, modulates the ohmic loss and therefore Joule's heating in the beams. This turns the beam to a thermal actuator generating a thermal actuation force component which can either amplify or attenuate the resonator vibration amplitude at resonance frequency depending on the polarity of the structural piezoresistive coefficient and thermal delays in the system. Previous results have proven that in case of constant current biased beams, in order for the extra thermal actuation force component to be in phase with the vibration of the resonator and hence amplify the vibration amplitude, longitudinal piezoresistive coefficient of the structural material should be negative [12]. Thus, in n-type single-crystalline silicon structures (negative piezoresistive coefficient), with adequate DC bias current flowing through an extensional mode beam, large vibration amplitudes can result from minute Lorentz actuation forces due to internal amplification of vibration amplitude. Figure 1 illustrates the interactions between the four physical domains (Magnetic, Mechanical, Electrical and Thermal) involved in the thermal-piezoresistive amplification process. The Lorentz force from an external magnetic field acting on a current carrying part of the resonator leads to an actuation force and therefore structural vibrations that are then internally amplified by the thermal-piezoresistive interactions within the extensional beam embedded in the structure.

In effect, the resonator absorbs energy from the DC bias source and uses it to partially compensate the mechanical losses that limit the vibration amplitude at resonance. Increasing the piezoresistor bias current increases the absorbed energy leading to further amplification (higher effective Q) and eventually even self-sustained oscillation of the resonator (absorbed energy larger or equal to mechanical losses). In this work, the above-mentioned principle has been utilized to amplify the displacement resulting from Lorentz actuation force and demonstrate ultra-high sensitivities to magnetic fields for such sensors.

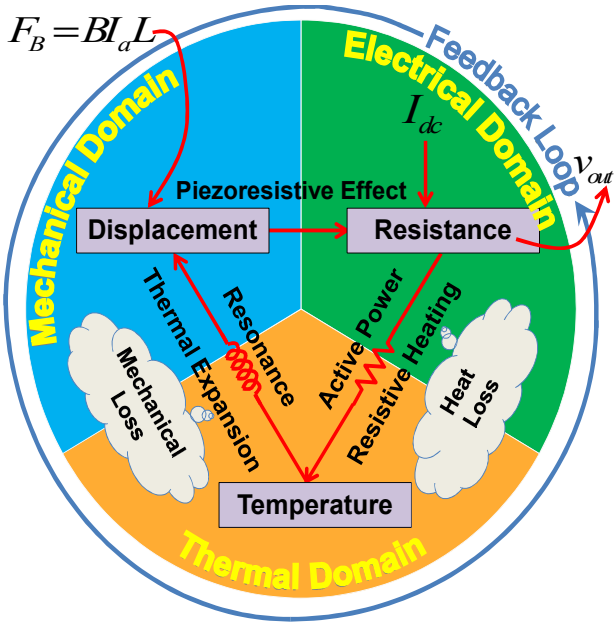

Figure 1: Schematic diagram showing interactions between different domains (Magnetic, Mechanical, Electrical and Thermal) in a Lorentz force magnetometer with thermal-piezoresistive internal amplification.

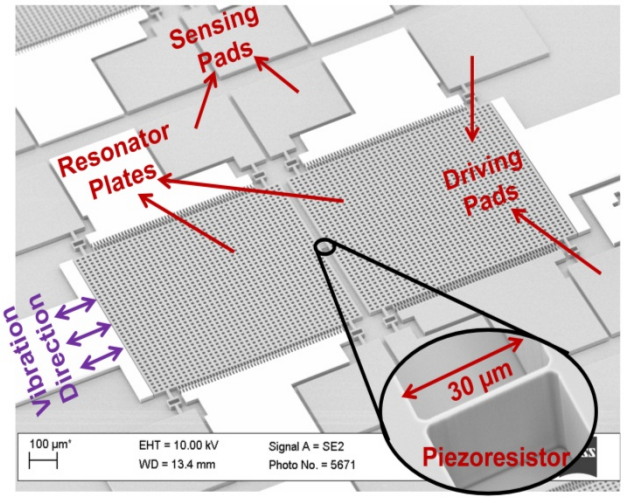

Figure 2: SEM view of the 400 kHz dual plate in-plane resonator. The inset shows a zoomed in view of the amplifying beam (piezoresistor-30 µm ×1.5 µm × 15 µm).

DEVICE DESCRIPTION

The dual plate monocrystalline silicon resonant structure of Figure 2 was fabricated on an SOI substrate (15µm thick device layer) using a single-mask micro-machining process and operated as a Lorentz Force Magnetometer. The resonator body was patterned and defined using deep reactive ion etching (DRIE) of silicon device layer and devices were released by removing the SOI buried oxide layer in hydrofluoric acid (HF). Holes on the resonator plates are provided to facilitate and accelerate undercutting of the large resonant plates.

The 30 µm long, 1.5 µm wide and 15 µm thick beam in the middle of the resonator connecting the two 400 µm × 400 µm resonator plates acts as the amplifying longitudinal beam. When the resonator resonates in its in-plane mode, this piezoresitor acts as a strain gauge that undergoes periodic tensile and compressive stress. The driving pads located on the two sides of the resonator plates are to generate the actuating Lorentz Force. Passing an AC current at the natural frequency of the resonator between the two driving pads results in a Lorentz Force that can actuate the resonator in its in-plane extensional mode. In this resonant mode, the resonator plates move back and forth as shown in Figure 3. The resulting vibration amplitude of the resonator due to the magnetically induced Lorentz Force is amplified by the mechanical Q of the resonator. The alternating stress in the piezoresistor beam leads to fluctuations in its electrical resistance. The sense pads connected to the two resonator plates are biased with a DC bias current which results in the internal amplification as discussed above. The same DC current also results in a modulated output voltage across the sense terminals which is proportional to the device vibration amplitude.

MEASUREMENT RESULTS

Measurement Setup

To test the resonator of Figure: 2 as a Lorentz Force MEMS magnetometer, a relatively long current carrying wire was placed next to the device which would act as the source of the magnetic field. The wire was kept at a specified distance from the device and in a direction such that the Lorentz Force from the applied magnetic field would actuate the resonator in its in-plane extensional mode. To avoid interference between the Lorentz force driving current and output signal of the device, a DC current was applied to the device for Lorentz force generation, and an AC magnetic field at the device resonant frequency was used to actuate the device. To generate the AC field, the RF output of the network analyzer was connected to the wire (P1 and P2- see Figure 3). The other advantage of using an AC field is that the device can operate without the interference from the Earth's magnetic field. A DC current I_{dc} passing through the silicon beam (P3 and P4- see Figure 3) allows piezoresistive readout of device resonance response (the same current is also responsible for internal amplification). Figure 3 shows the measurement setup and the electrical connections for device testing. The resonator frequency responses were obtained for different current amplitudes in the wire and for different the distances between the wire and the device which would in-turn change the magnitude of the magnetic field.

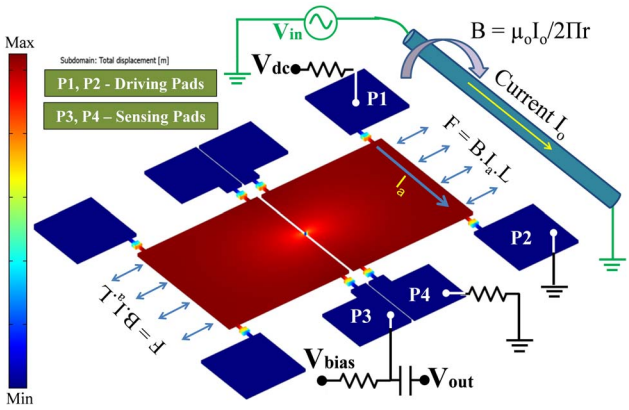

Figure 3: Finite element modal analysis of the resonator of Figure 2 showing the in-plane resonance mode and the measurement setup and its electrical connections.

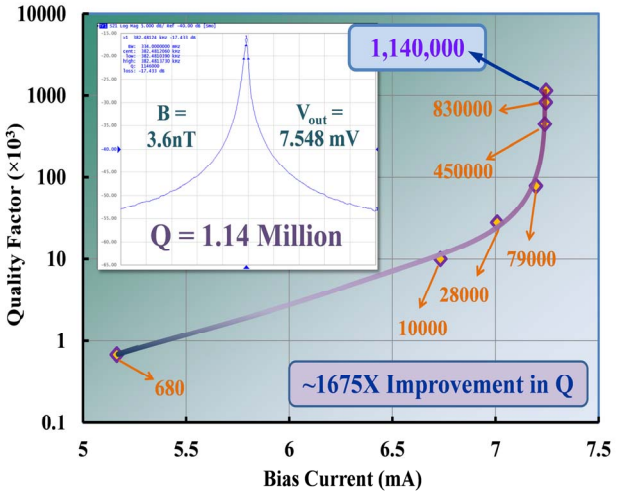

Figure 4: Graph showing measured effective Quality Factor versus the bias current demonstrating the Q and vibration amplification effect. Inset- Network Analyzer response for piezoresistor bias current of 7.245 mA.

Results

As the DC bias current between the sense pads increases, the onset of the internal thermal-piezoresistive amplification increases the vibration amplitude for the same actuating magnetic field. This effect shows up as an increase in the measured Q factor of the resonance peak in the device frequency response. Figure 4 shows the measured effective Quality Factor versus the bias current applied to the device demonstrating the amplification effect. The effective Q of the resonator increases from its intrinsic value of 680 (at 5.164 mA) to 1.14×10^6 (at 7.245 mA) under atmospheric pressure. The inset in Figure 4 shows the frequency response from the network analyzer for the magnetometer operating at 7.245 mA bias current with a magnetic field of 3.5 nT. An effective Q of 1.14×10^6 is obtained at this bias current and the measured output voltage is 7.548 mV. The maximum sensitivity (2.107mV/nT) of the magnetometer is achieved at this bias current. Figure 5(a) illustrates the frequency responses at field intensity of 3.5 nT for different piezoresistor bias currents showing how the output signal amplitude increases by increasing the bias current. Figure 5(b) illustrates the measured output voltage amplitudes (left y-axis) at resonance versus the magnitude of magnetic field (nT) for different bias currents. There is a ~2400X improvement in sensitivity (from 0.9 μV/nT to 2.107 mV/nT) when the bias current is increased from 5.164 mA to 7.245mA. The increase in output amplitudes (and thus sensitivity) at higher currents is partly due to higher piezoresistive sensitivity (higher piezoresistor bias current) and partly due to internal vibration amplification. To demonstrate the effect of internal amplification alone, sensitivity figure of merit (FOMS), defined as sensitivity divided by the bias current, is illustrated in Fig. 5 (b) (right y-axis) by the slope of the lines at different bias currents, showing a ~1620X improvement as a result of internal amplification alone. Figure 5(a) and 5(b) clearly shows that FOMS increases proportional to the resonator effective Q-factor as the bias current increases.

Noise and Limit of Detection

It should be noted that although the thermo-mechanical noise will also be amplified due to internal amplification, only noise components at close vicinity of the resonance frequency will be amplified by a factor close to the sensor output signal. Therefore, overall signal to noise ratio of the sensor is expected to improve. The minimum detectable magnetic field in such sensors is limited by different sources of noise including thermo-mechanical noise which is the most dominant component in micromechanical systems. The thermo-mechanical noise magnitude depends on the temperature and mechanical damping. To compare the amplification in noise due to the effect of thermal-piezoresistive amplification with the rate of the increase in signal, the noise behavior of the sensor was studied using a lock-in amplifier. For a bias current of 7.245mA, where the sensitivity of the device is maximum (2.1mV/nT), the noise floor is measured to be as low as 5.83 μV/√Hz, which translates to 2.8 pT/√Hz. The measurement results are summarized in Table 1, which highlights the Sensitivity, FOMS, effective Q and the Noise Floor values for different bias currents. Although it is evident from the Table that the noise amplitude will increase along with the signal amplification, overall signal to noise ratio (SNR) of the sensor improves with increase in bias current. Increasing the bias current leads to a temperature increase within the piezoresistor, thus raising the noise level, an increase in the signal level and the reduction in bandwidth at a higher pace will however result in the improvement in SNR.

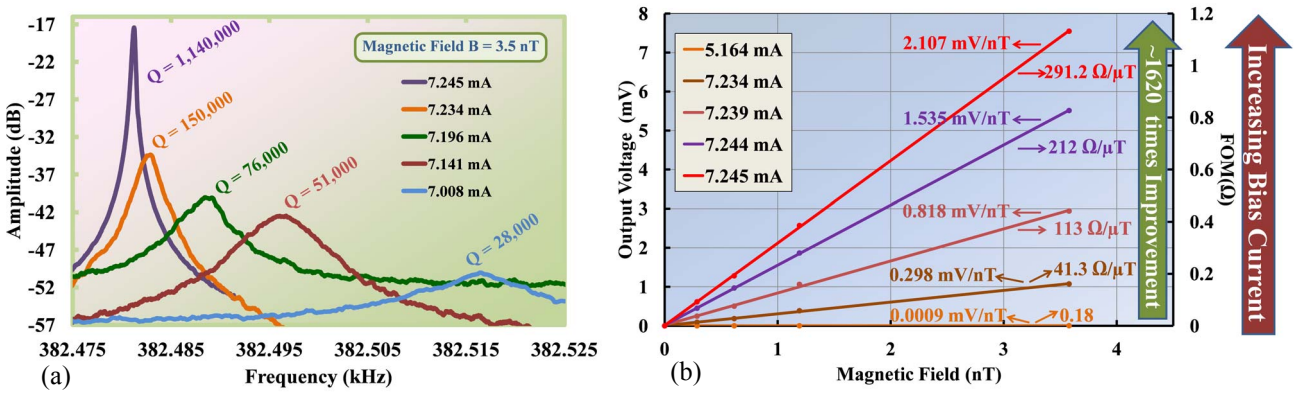

Figure 5: (a) Resonant responses of the device with different bias currents under constant magnetic field intensity of 3.5 nT. (b) Graph showing the output voltage amplitude and the FOMS values versus the magnetic field intensity for different bias currents.

Table 1: Sensitivity, FOMS Quality Factor and noise floor values for the magnetometer at different bias currents.

Bias Current (mA)	5.164	6.733	7.141	7.196	7.236	7.239	7.243	7.244	7.245
Sensitivity (μv/nT)	0.89	17.87	90.73	145.44	542.05	818.23	1188	1535.7	2107.8
FOMS (Ω/μT)	0.18	2.7	12.7	20.2	74.9	113	164	212	291.2
Quality Factor	680	1×10^4	2.8×10^4	7.9×10^4	28.5×10^4	45×10^4	6.3×10^5	8.3×10^5	1.1×10^6
Noise (pT/√Hz)	2340.3	264.64	61.71	39.34	10.72	7.11	4.90	3.79	2.76

CONCLUSION

Internal self amplification of a micro-scale resonant Lorentz Force magnetometer with piezoresistive readout was demonstrated. The sensitivity of the device made up of n-type silicon was improved by ~2400X. Close to ~1620X improvement in the magnetometer sensitivity figure of merit was validated. It is expected that by thinning down the piezoresistive amplifying beam and design optimizations, much higher sensitivities can be obtained potentially allowing compact low power sensor arrays for biomedical applications and brain mapping.

ACKNOWLEDGEMENTS

This work was supported by the US National Science Foundation under ECSS award #1345161.

REFERENCES

[1] D. Niarchos, "Magnetic MEMS: key issues and some applications," Sensors & Actuators A,Phys., Vol 106, no. ½, pp 255-262, Sep 2003.

[2] E. K. Ralph, "Comparison of a Proton and a Rubidium Magnetometer for Archaeological Prospecting," Archaeometry, vol. 7, no. 1, pp. 20–27, Jun. 1964.

[3] M. Li, V. T. Rouf, M. J. Thompson, and D. . Horsley, "Three-Axis Lorentz-Force Magnetic Sensor for Electronic Compass Applications," J. Microelectromechanical Syst., vol. 21, no. 4, pp. 1002–1010, Aug 2012.

[4] S. Levine, D. Silage, D. Henson, J. Y. Wang, J. Krieg, J. LaManca, and S. Levy, "Use of a triaxial magnetometer for respiratory measurements," J. Appl. Physiol. Bethesda Md 1985, vol. 70, no. 5, pp. 2311–2321, May 1991.

[5] J. Lenz and A. S. Edelstein, "Magnetic sensors and their applications," IEEE Sens. J., vol. 6, no. 3, pp. 631–649, Jun. 2006.

[6] A. Pérez Galván, B. Plaster, J. Boissevain, R. Carr, B. W. Filippone, M. P. Mendenhall, R. Schmid, R. Alarcon, and S. Balascuta, "High uniformity magnetic coil for search of neutron electric dipole moment," Nucl. Instrum. Methods Phys. Res. Sect. Accel. Spectrometers Detect. Assoc. Equip., vol. 660, no. 1, pp. 147–153, Dec. 2011.

[7] W. Zhang and J. E. Lee, "A horseshoe micromachined resonant magnetic field sensor with high quality factor," IEEE Electron Device Lett., vol. 34, no. 10, pp. 1310–1312, Oct. 2013.

[8] L.M. Miller, J.A. Podosek, E. Klruglick, "A μ-Magnetometer based on Electron Tunneling, Micro Electro Mechanical Systems, pp 467-472, Feb 1996.

[9] M. Thompson & D. Horsley, "Parametrically Amplified MEMS Magnetometer," IEEE Transducers, pp. 1194-1197, 2009.

[10] E. Mehdizadeh, V. Kumar, and S. Pourkamali, "Sensitivity Enhancement of Lorentz Force MEMS Resonant Magnetometers via Internal Thermal-Piezoresistive Amplification," IEEE Electron Device Lett., vol. 35, no. 2, pp. 268–270, Feb. 2014.

[11] E. Mehdizadeh, V. Kumar, and S. Pourkamali, "High Q Lorentz Force MEMS Magnetometer with Internal Self-Amplification," IEEE Sensors 2014, pp. 706–709, October 2014.

[12] A. Rahafrooz, and S. Pourkamali, "Thermal-piezoresistive energy pumps in micromechanical resonant structures," IEEE Trans. Electron Devices, vol. 59, no. 12, pp. 3587–3593, Dec. 2012.

CONTACT

V. Kumar, vxk120630@utdallas.edu
S. Pourkamali, siavash.pourkamali@utdallas.edu